

Paraelectric and ferroelectric order in two-state dipolar fluids

Dmitry V. Matyushov* and Andriy Okhrymovskyy

Department of Chemistry and Biochemistry, Arizona State University, PO Box 871604, Tempe, AZ 85287-1604

(Dated: November 20, 2018)

Monte Carlo simulations are used to examine cooperative creation of polar state in fluids of two-state particles with nonzero dipole in the excited state. With lowering temperature such systems undergo a second order transition from nonpolar to polar, paraelectric phase. The transition is accompanied by a dielectric anomaly of polarization susceptibility increasing by three orders of magnitude. The paraelectric phase is then followed by formation of a nematic ferroelectric which further freezes into an *fcc* ferroelectric crystal by a first order transition. A mean-field model of phase transitions is discussed.

PACS numbers:

In this Letter we describe Monte Carlo (MC) simulations of a fluid composed of two-state (TS) soft sphere (SS) particles interacting with the dipole-dipole potential. This model system, referred to as TS/SS fluid, shows a complex phase diagram including the transition from a nonpolar to polar, paraelectric phase followed by the transition to the ferroelectric phase. The existence of ferroelectric order in dipolar systems was first suggested by Debye¹ who predicted a transition at $y_c = 1$; $y = (4\pi/9)m^2\rho/kT$, where m is the dipole moment and ρ is the number density. Onsager² and Kirkwood³ have shifted the transition temperature to zero, $y_c \rightarrow \infty$. The generalized mean-field theory by Høye and Stell⁴ predicts $y_c = (1-\Theta)^{-1}$, $0 \leq \Theta \leq 1$ thus allowing transition at any temperature between the Debye and Onsager-Kirkwood limits. Recent computer simulations have indicated that isotropic ferroelectric phase is possible for polar fluids at a non-zero temperature,^{5,6,7} although the issue of boundary conditions is still debated.⁸ Most of the discussion of spontaneous order in dipolar systems has focused on systems with permanent dipoles. Real systems, either of molecular or nano-scale dimension, are composed of polarizable particles. The present simulations establish the existence of spontaneous ferroelectric order in polarizable dipolar fluids.

Many strongly dipolar states are created by intramolecular separation of charge, either thermal or optical, between the donor and acceptor parts of a molecule. Such states, common in chemistry and biology,⁹ often behave as independent donor-acceptor complexes with no cooperativity of charge-transfer transitions. A dramatic distinction from this situation is the Peierls instability in organic charge-transfer salts where charge-separated states are cooperatively created in one-dimensional stacks of donor and acceptor units.¹⁰ It appears that there is no fundamental reason why this type of transition should be limited to the crystal phase. We show that the cooperative coupling between TS dipoles leads to the nonpolar/polar second-order phase transi-

tion in the liquid phase.

The Hamiltonian of a fluid of TS/SS particles is

$$H = \sum_j H_{TS}(j) + \sum_{j<k} (u_{SS}(jk) - \hat{n}_j \mathbf{m}_j \cdot \mathbf{T}_{jk} \cdot \mathbf{m}_k \hat{n}_k). \quad (1)$$

Each individual particle j is characterized by the vacuum two-state Hamiltonian $H_{TS}(j)$ with the excited state population \hat{n}_j , the vacuum energy gap ΔI and the mixing between the states V . The dipole moment is zero in the vacuum ground state and is \mathbf{m} in the excited state. The excited-state dipoles interact via the dipole-dipole potential with $\mathbf{T}_{jk} = -\nabla_j \nabla_k |\mathbf{r}_j - \mathbf{r}_k|^{-1}$ in Eq. (1). Finally, the SS repulsion is

$$u_{SS}(jk) = 4\epsilon (\sigma/r_{jk})^{12}. \quad (2)$$

The model is characterized by the reduced density, $\rho^* = \rho\sigma^3$, reduced temperature, $T^* = kT/\epsilon$, and reduced dipole moment, $m^* = m/\sqrt{\epsilon\sigma^3}$. The reduced parameters for the TS system are: $V^* = V/kT$ and $I^* = \Delta I/kT$. The intermolecular interactions are fully characterized by two parameters: $x = (\rho^*)^4/T^*$ for SS repulsions¹¹ and y for dipolar coupling.

The exact calculation of the energies of N particles requires diagonalization of the $(2N)^2$ matrix. This is still prohibitively slow for condensed phase simulations. We will therefore use the Hartree decoupling assuming that the field acting on a given particle is produced by average excited-state populations of other particles.¹² The ground state energy of the fluid $E = \langle \prod_j \Psi_{gj} | H | \prod_k \Psi_{gk} \rangle$ is then defined on the wave functions Ψ_{gj} diagonalizing the Hamiltonian

$$H(j) = H_{TS}(j) - \hat{n}_j \mathbf{m}_j \cdot \mathbf{R}_j, \quad (3)$$

where

$$\mathbf{R}_j = \sum_k \mathbf{T}_{jk} \cdot \mathbf{m}_k \langle n_k \rangle \quad (4)$$

is the reaction field of the system dipoles. One gets

$$E = \sum_j E_g(j) + \sum_{j<k} (u_{SS}(jk) - u_{DD}(jk)). \quad (5)$$

*E-mail:dmitrym@asu.edu.

Here, the energy of each particle is

$$E_g(j) = \frac{1}{2} [\Delta I + u_{Rj} - \Delta E_j] \quad (6)$$

and the energy of the ground state in vacuum is set to be zero of energy. The energy gap $\Delta E_j = [(\Delta I + u_{Rj})^2 + 4V^2]^{1/2}$ in Eq. (6) is modulated by the coupling of the excited-state dipole \mathbf{m}_j to the reaction field, $u_{Rj} = -\mathbf{m}_j \cdot \mathbf{R}_j$. Finally, the excited-state population $2\langle n_j \rangle = 1 - (\Delta I + u_{Rj})/\Delta E_j$ defines the dipole moment $\boldsymbol{\mu}_j = \mathbf{m}_j \langle n_j \rangle$ in the dipole-dipole interaction potential in Eq. (5): $u_{DD}(jk) = -\boldsymbol{\mu}_j \cdot \mathbf{T}_{jk} \cdot \boldsymbol{\mu}_k$. The dipole moment of each particle thus fluctuates with the instantaneous value of the reaction field.

The MC simulations of TS/SS fluids were performed for the NVT ensemble of $N = 256$ particles in a cubic box with periodic boundary conditions. The long range dipolar interactions were accounted for by the reaction field method with infinite reaction field dielectric constant. An MC trial move combines displacement and rotation of a particle followed by iterative, self-consistent calculation of the fields \mathbf{R}_j .¹³ Each trial move thus results in a new set of dipoles $\boldsymbol{\mu}_j$. This calculation is the most time-consuming part of the simulation protocol. Typical simulations were 8×10^5 cycles long (170 h on a single Alpha/740MHz processor), points close to phase transitions required simulations with 1.2×10^6 cycles.

The appearance of the nonpolar/polar (NP) and polar/ferroelectric (PF) transitions was monitored by calculating the polar order parameter $P = \langle \mu \rangle / m = (Nm)^{-1} \langle \sum_j \mu_j \rangle$ and the usual orientational first-order (ferroelectric) and second-order (nematic) parameters, S_1 and S_2 , respectively.^{5,14} The isotropic, nonpolar phase is characterized by all order parameters equal to zero. The polar state is marked by $P \neq 0$, whereas P , S_1 , and S_2 are all non-zero in the ferroelectric nematic.

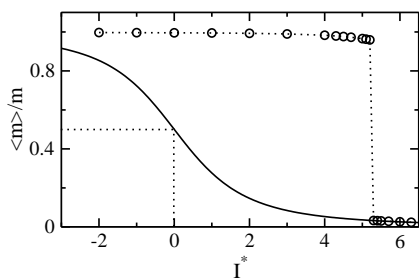


FIG. 1: Polar order parameter of non-interacting particles (line) and of the TS/SS fluid (points) vs the reduced vacuum energy gap $I^* = \Delta I/kT$; $\rho^* = 0.8$, $m^* = 2.0$, $T^* = 0.8$. The dashed line indicate the point $\langle \mu \rangle / m = 1/2$ at $I^* = 0$, the dotted line connects the simulation points.

Spontaneous creation of a non-zero average dipole moment is a result of cooperative coupling between induced dipoles. The dipole moment μ of an isolated particle changes smoothly with the energy gap I^* reaching one half of its maximum value m at zero gap $I^* = 0$ (Fig. 1).

This point corresponds to a purely covalent state of the donor-acceptor complex. The ionic character, $\mu/m \simeq 1$, is achieved at $I^* < 0$, $|I^*/V^*| \gg 1$. In contrast, when the particles are allowed to interact in the fluid phase, cooperativity results in a very sharp change of $\langle \mu \rangle$ from zero to m at the transition value $I_{NP}^* > 0$ (Fig. 1, $I_{NP}^* = 5.2$ at $\rho^* = 0.8$, $T^* = 0.8$, $m^* = 2.0$, and $V^* = -1.0$). Thermal fluctuations of induced dipoles thus reinforce each other leading to a negative energy of interaction with the reaction field, $\langle u_R \rangle < 0$, which overrides the positive vacuum energy gap and the polarization energy invested in creating the dipole.

This type of transition was predicted by Logan^{15,16} who suggested that a solution of alkali atoms can show a continuous transition from a normal insulator (non-polar) to excitonic insulator (paraelectric) phase.^{12,17,18} Although the atomic dipole is created by hybridizing the non-polar atomic states through the transition dipole, the basic physics of reaction-field stabilization overriding the energy gap^{19,20} is common to the present problem and the excitonic insulator transition. It is interesting to note that non-linear polarizability effects characteristic of the two-state description might be important for the transition to occur since the complex phase diagram obtained here for the TS/SS fluid does not exist for the fluid of Drude oscillators often used to model atomic and molecular polarizability.²¹

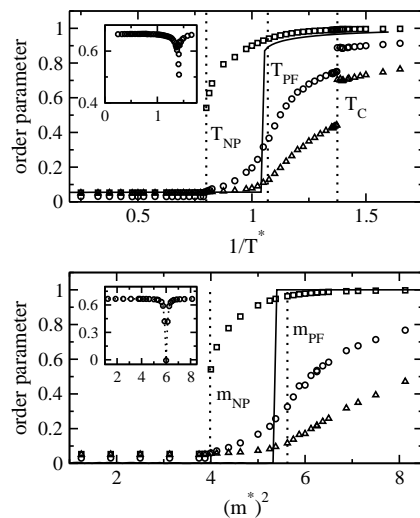


FIG. 2: Order parameters P (squares), S_1 (circles), and S_2 (triangles) of TS/SS fluids vs $1/T^*$ (upper panel, $m^* = 2.0$) and vs $(m^*)^2$ (lower panel, $T^* = 1.25$) at $\rho^* = 0.8$, $I^* = 4.0$, $V^* = -1.0$. The solid lines show the results of mean-field theory calculations [Eqs. (7)–(11)] for the order parameter P . The Binder parameter,²³ $1 - \langle E^4 \rangle / 3\langle E^2 \rangle^2$, vs $1/T^*$ (upper panel) and vs $(m^*)^2$ (lower panel) is shown in the insets.

The MC simulations shown below consider the variation of intermolecular repulsion and attraction through T^* and m^* at constant ρ^* , I^* , and V^* . Three order parameters as functions of T^* and m^* are shown in Fig. 2. The parameter P increases sharply at T_{NP}^*/m_{NP}^* mark-

ing the onset of the polar (paraelectric) phase. Both S_1 and S_2 start to increase with decreasing temperature or increasing dipole moment resulting in the PF transition at T_{PF}^*/m_{PF}^* . The latter point is defined from the peak of dielectric susceptibility (Fig. 3, the simulation data corresponding to the change of m^* at constant T^* are not shown). A similar susceptibility peak was observed for the PF transition in a fluid of hard sphere Ising spins with a square-well attraction.²²

Finally, both S_1 and S_2 have a discontinuous jump at $T_C^* = 0.73$. The analysis of the density structure factors and pair distribution functions indicates that the system is in fluid phase above T_C and freezes into the *fcc* ferroelectric at T_C . Further, the phase between T_{PF} and T_C is a ferroelectric nematic as is seen from the analysis of angular projections of the pair distribution function and from the analysis of the position distribution functions parallel and perpendicular to the director (not shown here). These functions show no indication of spatial structure thus ruling out a possibility of smectic order. No crystallization was achieved by changing m^* at constant T^* in the range of values studied.

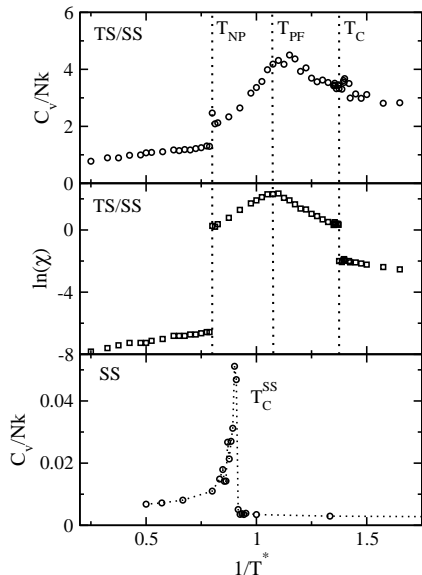


FIG. 3: Heat capacity C_v (upper panel) and polarization susceptibility χ (middle panel) of the TS/SS fluid and heat capacity of the SS fluid (bottom panel). $m^* = 2.0$, $I^* = 4.0$, $V^* = -1.0$ for the TS/SS fluid, $\rho^* = 0.8$ for both the TS/SS and SS fluids. MC simulations of the SS fluid were performed with $N = 2048$ particles in the box. The typical simulation length was 50 000 cycles.

The NP transition is characterized by discontinuity of the heat capacity $C_v/Nk = \langle(\delta E)^2\rangle/N(kT)^2$ and a very substantial (3 orders of magnitude) increase in the dielectric susceptibility $\chi = \rho\langle(\delta\mathbf{M})^2\rangle/NkT$, where $\delta\mathbf{M}$ is the fluctuation of the total dipole of the system of N particles (Fig. 3). At the same time, the total energy is continuous pointing to a second-order phase transition (Fig. 4). The PF transition is continuous both in energy and heat ca-

capacity and is manifested by maxima of C_v and χ (Fig. 3). Finally, crystallization is a first-order transition with the latent heat arising mostly from the change in the dipolar interaction energy. The continuous character of the NP and PF transitions is supported by the value of the Binder parameter,²³ $1 - \langle E^4 \rangle / 3 \langle E^2 \rangle^2$, which is very close to $2/3$ (continuous transition) in the entire range of parameters except at crystallization when it takes a dip consistent with the first order of this transition. The onset of the polar phase is also marked by a continuous increase in the average reaction field and a discontinuous jump in its variance (Fig. 4, bottom panel). The breakdown of the linear response approximation, $-kT\langle u_R \rangle = \langle(\delta u_R)^2\rangle$, at the onset of paraelectric phase²⁰ is characteristic of polarizable systems.²¹

The temperature of NP transition falls in the region of freezing transition of the reference fluid with the repulsive potential $U_{SS} = \sum_{j < k} u_{SS}(r_{jk})$ which is characterized by a peak of the heat capacity $C_v/Nk = \langle(\delta U_{SS})^2\rangle/N(kT)^2$ (bottom panel in Fig. 3). The SS fluid crystallizes into an *fcc* lattice below the transition temperature T_C^{SS} as we found from the density structure factors in accord with previous reports in the literature.²⁴ It may be suggested that positional instabilities of the reference repulsive potential drive the PF transition of the TS/SS fluid. However, dipolar interactions do not favor the highly symmetric *fcc* lattice,²⁵ and the system stays in the fluid phase in the temperature range $T_{PF} \leq T \leq T_C$ crystallizing at T_C . This interpretation is consistent with the notion advocated by several authors²⁵ that dipoles suppress freezing into a high-symmetry lattice due to the anisotropic nature of dipolar forces. Note that the *fcc* lattice does not necessarily represent the ground state since a ferroelectric solid can never be strictly cubic. Other stable structures may be suppressed in simulations by the cubic shape of the simulation cell and periodic boundary conditions.⁶

The energy per particle $e = E/NkT$ depends on the fluctuating variable $u = u_R/kT$. The mean-field solution, neglecting these fluctuations, is given as

$$\langle e \rangle = (P/2)\langle u \rangle - P\Delta e(\langle u \rangle), \quad (7)$$

where $\Delta e = \Delta E/kT$. The average $\langle u \rangle$ is affected by the macroscopic reaction field

$$\mathbf{R}_0 = (4\pi/3)m\rho P S_1(1 - \Theta)\hat{\mathbf{d}} \quad (8)$$

caused by spontaneous ferroelectric polarization of the liquid and the microscopic reaction field \mathbf{R}_{mic} due to dipole-dipole correlations. Here, Θ is the mean-field parameter of Høye and Stell^{4,26} correcting the macroscopic field by the account of local dipolar correlations. If one assumes that the microscopic correlations are not affected by the macroscopic order, $\langle u \rangle$ becomes

$$\langle u \rangle = 3yP(1 - \Theta)S_1^2 - (2/P)u_D(\langle \mu \rangle), \quad (9)$$

where $u_D(\langle \mu \rangle) = -\beta\langle \mu \rangle \cdot \mathbf{R}_{mic}/2$ is the reduced average interaction energy between particles carrying the average

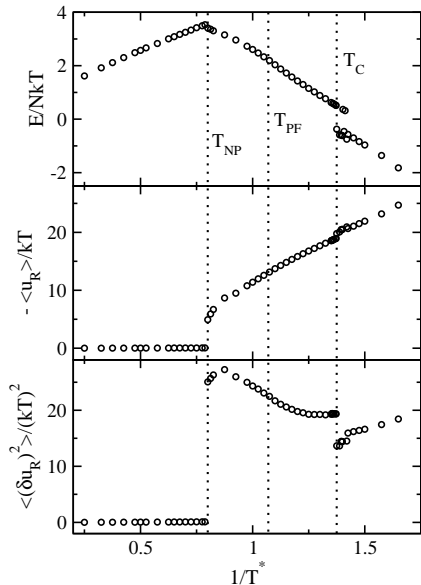


FIG. 4: Total average energy per particle, E/NkT , the energy of dipolar coupling to the reaction field, $-\langle u_R \rangle$, and its variance, $\langle (\delta u_R)^2 \rangle$, vs $1/T^*$ for the TS/SS fluid: $\rho^* = 0.8$, $m^* = 2.0$, $I^* = 4.0$, $V^* = -1.0$.

dipole $\langle \mu \rangle = Pm$. Such dipolar interactions are well described by the Padé-truncated perturbation expansion²⁷ resulting in the following free energy per particle

$$f_D/kT = -\frac{y^2 P^4 I_2(x)}{1 + yP^2 I_3(x)/I_2(x)}. \quad (10)$$

The perturbation integrals in Eq. (10) are defined on the reference SS fluid as

$$\begin{aligned} I_2(x) &= (27/128\pi^2) \langle (\rho^2 r^6)^{-1} \rangle_{SS}, \\ I_3(x) &= (27/512\pi^3) \langle \rho^3 W_{DDD} \rangle_{SS}, \end{aligned} \quad (11)$$

where W_{DDD} is the Axilrod-Teller potential.¹⁴ The average over the configuration of the SS fluid, $\langle \dots \rangle_{SS}$, has been calculated from MC simulations. $I_2(x)$ and $I_3(x)$ obtained from simulations at different temperatures and densities all fall on one universal dependence on x . However, the scaling $I_2(x) \propto x^{-0.5}$ and $I_3(x) \propto x^{-0.75}$ predicted from the statistical average is not seen in the simulations. Instead, much weaker power laws, $I_2(x) = 0.1433x^{-0.138}$ and $I_3(x) = 0.0314x^{-0.09915}$, fit the data. The perturbation integrals obtained at different ρ^* and T^* are smooth functions of x up to $\rho^* = 0.9$.

The paraelectric order parameter can be calculated with the mean-field solution for $\langle u \rangle$ and the free energy obtained by thermodynamic integration of $\langle e \rangle$ in Eq. (7). The mean-field solution does not reproduce the separation of the NP and PF transitions and instead gives a direct transition from a non-polar phase to a polar, ferroelectric phase at a single transition point. The calculation shown in Fig. 2 is performed for the Θ parameter in Eq. (8) from the mean-spherical solution for hard dipolar spheres.^{4,28} The agreement with simulations for the PF transition is very good for both the dependence on temperature (upper panel in Fig. 2) and the dependence on the dipole moment (lower panel in Fig. 2). A model including fluctuations of the reaction field²⁹ may result in a more accurate description of the NP and PF transitions yielding a separate paraelectric phase.

Acknowledgments

This work was supported by the NSF (CHE-0304694).

-
- ¹ P. Debye, Phys. Z. **13**, 97 (1912).
² L. Onsager, J. Am. Chem. Soc. **58**, 1486 (1936).
³ J. G. Kirkwood, J. Chem. Phys. **7**, 911 (1939).
⁴ J. S. Høye and G. Stell, J. Chem. Phys. **64**, 1952 (1976).
⁵ D. Wei and G. N. Patey, Phys. Rev. Lett. **68**, 2043 (1992).
⁶ G. T. Gao and X. C. Zeng, Phys. Rev. E **61**, R2188 (2000).
⁷ G. Ayton and G. N. Patey, Phys. Rev. Lett. **76**, 239 (1996).
⁸ D. Wei, G. N. Patey, and A. Perera, Phys. Rev. E **47**, 506 (1993).
⁹ R. A. Marcus, Rev. Mod. Phys. **65**, 599 (1993).
¹⁰ Z. G. Soos, Annu. Rev. Phys. Chem. **25**, 121 (1974).
¹¹ J.-P. Hansen, Phys. Rev. A **2**, 221 (1970).
¹² M. D. Winn and D. E. Logan, J. Phys.: Condens. Matter **4**, 5509 (1992).
¹³ F. J. Vesely, J. Comp. Phys. **24**, 361 (1976).
¹⁴ M. P. Allen and D. J. Tildesley, *Computer simulation of liquids* (Clarendon Press, Oxford, 1996).
¹⁵ D. E. Logan, Phys. Rev. Lett. **57**, 782 (1986).
¹⁶ D. E. Logan, J. Chem. Phys. **86**, 234 (1987).
¹⁷ R. W. Hall and P. G. Wolynes, Phys. Rev. B **33**, 7879 (1986).
¹⁸ B.-C. Xu and R. M. Stratt, J. Chem. Phys. **89**, 7388 (1988).
¹⁹ E. S. Fois and A. Gamba, J. Chem. Phys. **100**, 9044 (1994).
²⁰ R. Spezia, C. Nicolas, and A. Boutin, Phys. Rev. Lett. **91**, 208304 (2003).
²¹ S. Gupta and D. V. Matyushov, J. Phys. Chem. A **108**, 2087 (2004).
²² P. Ballone, P. de Smedt, J. L. Lebowitz, J. Talbot, and E. Waisman, Phys. Rev. A **35**, 942 (1987).
²³ K. Binder and D. W. Heermann, *Monte Carlo Simulation in Statistical Physics* (Springer-Verlag, Berlin, 1992).
²⁴ B. B. Laird and D. M. Kroll, Phys. Rev. A **42**, 4810 (1990).
²⁵ B. Groh and S. Dietrich, Phys. Rev. E **63**, 021203 (2001).
²⁶ J. S. Høye and G. Stell, Mol. Phys. **86**, 707 (1995).
²⁷ C. G. Gray and K. E. Gubbins, *Theory of molecular liquids* (Clarendon Press, Oxford, 1984).
²⁸ M. S. Wertheim, J. Chem. Phys. **55**, 4291 (1971).

²⁹ H. Zhang and M. Widom, Phys. Rev. B **51**, 8951 (1995).